Development of a novel electroless deposited nickel braze for micro-tubular solid oxide fuel cell current collector contacting

Item Type	Journal article
Authors	Hodjati-Pugh, O;Dhir, A;Steinberger-Wilckens, R
Citation	Hodjati-Pugh O, Dhir A, Steinberger-Wilckens R. (2021) Development of a novel electroless deposited nickel braze for micro-tubular solid oxide fuel cell current collector contacting. Journal of Advanced Joining Processes, 4, 100070.
DOI	10.1016/j.jajp.2021.100070
Publisher	Elsevier
Journal	Journal of Advanced Joining Processes
Download date	2025-05-19 09:18:07
License	https://creativecommons.org/licenses/by-nc-nd/4.0/
Link to Item	http://hdl.handle.net/2436/624417

Development of a novel electroless deposited nickel braze for micro-tubular solid oxide fuel cell current collector contacting

O. Hodjati-Pugh [a,*], A. Dhir [b], R. Steinberger-Wilckens [a]

[a] *Centre for Fuel Cell and Hydrogen Research, School of Chemical Engineering, University of Birmingham, B15 2TT*
[b] *School of Chemical Engineering, University of Wolverhampton, WV1 1LY*

ARTICLE INFO

ABSTRACT

A brazing process for the fuel electrode (anode) contacting of a micro-tubular fuel cell is reported. The low-cost, novel, electroless deposited braze suitable for mass production was optimised with respect to material loading and brazing environment. Durable current collector-anode joints were obtained while protecting sensitive solid oxide fuel cell components. It was determined that a minimum braze loading of 20 μm thickness was required to join the current collector at multiple contacts along the interior tube wall. The final brazed current collector design achieved a high peak power density of 0.14 W.cm^{-2} at 750°C, 2.35 times higher than for the un-brazed design.

Introduction

Solid oxide fuel cells (SOFC) are highly efficient electrochemical conversion devices capable of delivering electrical efficiency of 50 to 60% and above (Larmine and Dicks, 2006). Provided the heat produced by the SOFC can be deemed as useful, a combined heat and power (CHP) efficiency of more than 85% can be attained (Mench, 2008). Fuel cells are a 'zero emission' technology provided they are fuelled with renewably sourced fuels with no fossil carbon content (e.g. green hydrogen) (O'Hayre et al., 2009). High temperature fuel cells such as SOFCs have a higher tolerance to fuel impurities and can operate on hydrocarbons such as for example biogas, alleviating complexities surrounding hydrogen supply infrastructure (Kendall et al., 2016). Microtubular solid oxide fuel cells (μT-SOFC) have inherently superior thermo-mechanical durability, short start-up times, and relatively high stack power density versus planar devices (Bujalski et al., 2007, Kendall, 2016). This lends them for use in portable devices such as phone chargers, laptops, auxiliary power units, and electrically powered drones, to name but a few applications (Kendall et al., 2016, Meadowcroft et al., 2013, Fernandes et al., 2018, Lee et al., 2008).

High ohmic polarisation arising from long axial (and to a lesser extent radial) conduction pathways constitutes a bottleneck in μT-SOFC technology (Boersma et al., 2000, Panthi and Tsutsumi, 2014). An optimised current collector/interconnect design is the main tool in reducing the ohmic polarisation through the minimisation of the average conduction path length (Hodjati-Pugh et al., 2021). The current collector itself must have a low ohmic contribution and a low contact resistance at the interface(s) with the electrode.

Collecting current internally (on the bore side) of an anode supported μT-SOFC such as the brush-like design seen in Fig. 1 presents several advantages over the state-of-the-art external current collector configuration. An external anode current collector requires the removal of fuel cell layers to expose the anode from the cell exterior (Dhir and Kendall, 2008). This is labour intensive, compromises the mechanical integrity of the cell and reduces the available active area for current production and thus the total power produced per cell. This is exacerbated if multiple current collectors are required to reduce the current path length (Bai et al., 2011). An internal current collector allows collecting current from multiple locations along the interior anode wall, which increases the contact area and reduces the current path length. However, the internal current collector must not impede the fuel flow through the tube and in/out of the electrodes to the extent where performance is negatively affected (Hodjati-Pugh et al., 2021).

Securing an internal current collector to the electrode is more complex than an external current collector which can rely on mechanical force (such as tying) or contacting pastes/adhesives (Majewski and Dhir, 2018). The narrow tube bore and high length-to-diameter ratio of μT-SOFCs lead to difficult access for the application of contact materials. Relying on the current collector materials' elasticity for maintaining contact to the anode is not sufficient for high temperature operation and

---

research has shown this leads to sagging and an increase in contact resistance (Dhir and Kendall, 2007, Hodjati-Pugh et al., 2021). This effect is magnified when the µT-SOFC internal diameter increases and when a cell undergoes thermal cycling (Meadowcroft et al., 2014). The loss of contact of µT-SOFC internal current collector poses performance and durability concerns and must be addressed.

The state-of-the-art µT-SOFC anode current collectors are metallic, made of silver, nickel, gold, platinum or stainless steels (Fergus, 2005). Techniques such as welding that are typically used for contacting/joining metals are not compatible with fuel cells and will either not join the components and/or lead to damage to the fuel cell, for example from thermal shock (Kendall et al., 2016). However, furnace brazing was identified as a suitable candidate process for joining the current collector to the SOFC electrode. The brazing environment can be controlled to promote joint formation, strength, durability, and conductivity. The environment can also be controlled to protect the substrate material. Common brazing environments are reducing, inert, or under a strong vacuum (Kim et al., 2009). Avoiding oxide formation on the substrate and joint is particularly important for brazing metals. Silver/copper braze alloys with moderate joint strengths were developed for use with perovskite ceramics by Erskine et al. (Erskine et al., 2002). Although this research was not fuel cell specific, it was an early indication (2002) that brazing of a perovskite cathode to a cathode current collector was feasible.

SOFC brazing

The very few literature articles on brazing in the field of µT-SOFC indicated that brazing was possible but more research was needed to develop brazing for current collector contacting which the current study aims to address. There have been several studies on brazing in SOFC technology, however, brazing is primarily used for sealing with several developers using brazing for current collector contacting (Mahato et al., 2015, Tucker et al., 2006, Chao et al., 2016, Sammes et al., 2005).

Kim et al. (Kim et al., 2009) used induction brazing to join the Ni-YSZ anode and YSZ electrolyte of an anode supported tubular cell to a ferritic stainless steel metallic cap (SUS430). The steel cap was used as a manifold, joined to the YSZ electrolyte, and as an anode current collector joined to the Ni-YSZ support. Four braze materials were trialled, two nickel based brazes, namely BNi-2 and BNi-5, and two silver-copper based brazes, namely Nicusil 8 and Palcusil 10. When the braze was used as a sealant, the nickel based braze materials outperformed the silver-copper based braze materials with respect to the permeability of helium. The BNi-2 was the best performing and had a permeability of 1 $\times$ 10^{-6} l.cm^{-2}.s^{-1} at a differential pressure of 3 atm. This was determined to be as a result of superior wetting and flow of the BNi-2 around a round surface. A four-probe electrical conductivity test was used on the tubular fuel cells with the BNi-2 and BNi-5 braze as a current collector contact material. The conductivity of the cell at 750°C with BNi-2 was 450 S. cm^{-1}, 80% higher than the BNi-5 cell at 250 S.cm^{-1}. The 11.2 cm^2 cell was fed with 50 ml.min^{-1} of H_2 at 750°C. The cell had a current density at 0.7 V of 0.2 A.cm^{-2}, a peak power density of 0.21 W.cm^{-2}, and an estimated ASR from the polarisation curve of 1.1 Ω.cm^2 at 750°C. The OCV was greater than 1 V, indicating all joints were gas tight, meaning the BNi-2 worked well as a manifold sealant. The durability of the fuel cell with the BNi-2 braze in both oxidising and reducing atmosphere was indicated by its stable conductivity values over the 6 days of testing.

Experimental

Brazing apparatus

Brazing was conducted in-house in inert and reducing environments using an Elite tubular furnace, brazing chamber, and gas supply. A brazing rig process and instrumentation diagram of the in-house brazing rig was described previously in (Hodjati-Pugh et al., 2019). Inert brazing was conducted using argon while reducing brazing was achieved with a flow of 4% H_2 in argon.

A reducing environment cleans/reduces the oxides that are usually present on the parent materials to be joined and aids the wetting/bonding which again promotes joint strength. An inert environment eliminates the potential for oxidation of the braze and braze components and can be used when a reducing environment would be detrimental to the parent materials, as for instance the cathode material of the µT-SOFC cell.

µT-SOFC and internal current collector

The Ni-YSZ anode supported µT-SOFC used in this study, the internal current collector named hiTRAN® and its implementation as a current collector were previously detailed in (Hodjati-Pugh et al., 2019). The µT-SOFC had an external diameter of 6.8 mm, an internal diameter of 5.5 mm and an active area of 20 cm^2. The internal current collector was a brush-like device adapted from heat exchanger turbuliser technology made by CALGAVIN Ltd. The hiTRAN® turbuliser can be made of various metals (nickel in this study) and has a central core that supports a 100 mm section of coils that span the entirety electrode surface beneath the cathode, subsequently feeding the electrons where they are produced into the central core wire to be extracted to the external circuit. The hiTRAN® was oversized with respect to the tube bore size and upon installation was a tight fit (approx. 80 N). However, it was shown previously that the force was 10 times lower after just four hours of operation at 750°C, increasing contact resistance and decreasing contact area significantly. The design was deemed not suitable for a durable and portable µT-SOFC powered device and that current collector contacting via brazing was required (Hodjati-Pugh et al., 2019). The cathode
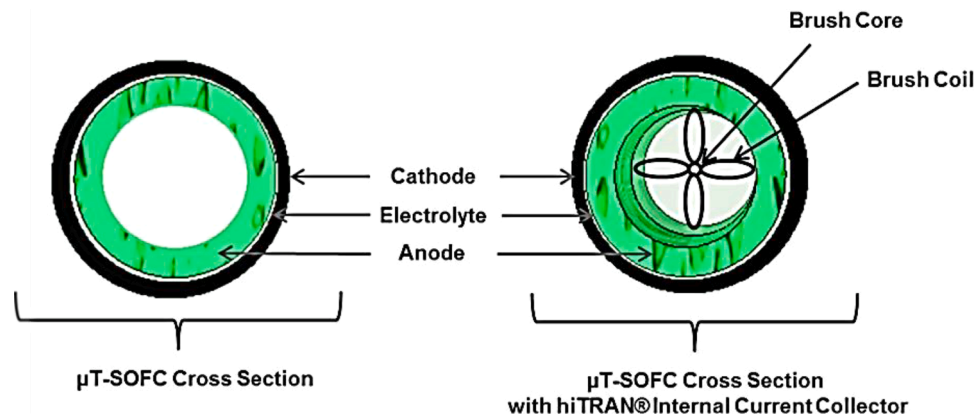

Fig. 1. µT-SOFC cross-section schematic with and without hiTRAN® internal current collector used in this study.

current collector, on the other hand, had a spine wire running down its length with tie wires to secure it and collect current circumferentially. The cathode wires were silver and were used in conjunction with a porous silver contacting paste.

Electroless nickel-alloy braze

To achieve a homogeneous distribution of braze material that would not become dislodged upon assembly, electroless plating was explored. Electroless plating is common in the automotive and electronics sectors for electrical contacts/switches and printed circuit boards. Nickel plating is typically used for wear resistance, hardness and for corrosion resistance. Electroless deposition is a chemical reduction process that does not require a current as is used in electroplating processes. Fine control of deposition thickness can be achieved as well as superior uniformity, regardless of geometry, with respect to electrolytic processes. Parts are dipped into a bath with the nickel based plating solution and a reducing agent, adjusting the exposure time to control the deposition thickness (Sudagar et al., 2013). Phosphorus is added at a mass fraction of between 2 and 14% to provide wear resistance, improve hardness, provide corrosion protection, and modify electrical properties. The plating chemistry is available with phosphorous levels in a low (2 to 5 wt%), medium (5 to 11 wt%) and high (11 to 14 wt%) quantity. The coating density and wear resistance increase with increasing phosphorous content while hardness reduces. Noting the compositional similarity of the medium content electroless nickel (EN) coating to the BNi-7 braze material as seen in Table 1, the EN coating was selected as a candidate for brazing.

For use as a braze material, the primary function of the phosphorous was for its use as a melting point depressant as used in typical braze materials. The correct content being crucial to enable the nickel based EN braze deposited on the hiTRAN® to pass the liquidus temperature and become mobile before reaching the melting point of the nickel hiTRAN® support itself. Increasing the phosphorous content decreases the melting point from around 1200°C for low phosphorous alloys to 800°C for high phosphorous content alloys seen in Fig. 2 (a). Given the application in interconnection, consideration had to be made to the conductivity of the joint as increasing phosphorous content also increased electrical resistivity as seen in Fig. 2 (b) (Parkinson, 1997).

The content of the phosphorous was chosen to be similar to that of BNi-7. The solution was estimated at 6 to 9 wt% phosphorous content which brought the melting range to between 900°C and 1100°C. A comparison of the EN braze and BNi-7 braze properties and braze temperature is seen in Table 1. Two coating thicknesses of 10 μm and 20 μm were trialled. Plating was provided by Frost Electroplating Ltd based in Birmingham. The hiTRAN® was weighed before and after the 20 μm EN braze was applied, evidencing a braze mass of 0.18 g $\pm$ 0.02 g. The low variance was indicative of the fine control over braze loading of electroless plating EN.

Brazing profile

The brazing temperature was chosen as 1065°C for both brazing environments. A fast ramp of 10 K.min^{-1} was set from room temperature to 800°C, while a slow ramp of 2 K.min^{-1} was chosen between 800°C and the brazing temperature to minimise stress in the fuel cell, hiTRAN® and braze material. For both inert/reducing brazing, a high gas flow of 500 ml.min^{-1} was introduced for 5 minutes before heating commenced

with backpressure purges, ensuring the removal of air from the chamber. A lower 300 ml.min^{-1} gas flow was used during the brazing process.

Results and discussion – electrochemical testing

Fig. 3 shows the contribution of the ohmic resistance and cell resistance to the total cell resistance (the sum of the ohmic and electrode polarisation resistance contributions) for the hiTRAN® turbuliser as a current collector. The variants shown are un-brazed, compared with 10 μm and 20 μm electroless coatings of EN material brazed under reducing atmosphere, and with 20 μm coating of EN brazed under an inert atmosphere. The impedance was measured at 0.7 V in the ohmic loss dominated region. The ohmic polarisation of the 10 μm EN layer brazed in reducing conditions increased by 19% compared to the un-brazed value. This was due to an increase in the current collector contact resistance. The hiTRAN-anode-braze interfaces will successfully join/braze provided there is sufficient amount of braze. The 10 μm coating was not enough in quantity to flow to the hiTRAN-anode interface, wet both the parent materials, and then cool to form a joint. The failed attempt at a 10 μm braze thickness was indeed a high-temperature thermal cycle. This promoted the separation of the hiTRAN® from the anode as a result of the softening of the nickel and the mismatch in CTE between the nickel hiTRAN® turbuliser and the fuel cell. The ohmic polarisation value increased as the hiTRAN® element separated from the wall, increasing the contact resistance due to the decreasing number of contact points and diminished contact force at the anode-hiTRAN® interfaces. The un-brazed cell was not subject to a high-temperature brazing thermal cycle and thus subject to less stress. The aforementioned resulted in the un-brazed cell having a lower polarisation resistance and electrically/electrochemically outperforming the cell with the failed 10 μm brazing.

The ohmic polarisation was reduced from 0.231 Ω for the un-brazed hiTRAN® turbuliser to 0.079 Ω and 0.090 Ω for the thicker 20 μm EN coating brazed under reducing conditions, and 20 μm EN brazed in inert atmosphere, respectively. This corresponded to ohmic polarisation values of 34% and 39% compared to the un-brazed value, respectively. This indicated that these brazing materials and techniques were successful in forming joints. A comparison of ohmic polarisation values of the 20 μm EN plated elements indicated that the process supplied better properties when brazing in a reducing environment. This promoted the formation of an oxide-free joint with increased joint strength (and most likely durability) (Sekulic, 2013).

The electrode polarisation of all cells with brazed turbulisers increased versus the un-brazed samples. The electrode polarisation of the un-brazed hiTRAN® elements was 0.011 Ω, increasing to 0.067 Ω, 0.061 Ω and 0.019 Ω for the 10μm and 20μm EN plated hiTRAN® brazed in reducing conditions, and 20μm EN hiTRAN® brazed in inert conditions, respectively. Upon visual inspection of the cells brazed in a reducing environment, the anode colour had remained unchanged throughout the brazing process indicating re-oxidation had not occurred. However, some minor delamination of the cathode was evident, although the majority of the material had remained intact. The delamination was not evident in the cells brazed in an inert environment. This indicated the cathode delamination was a result of the environment rather than the furnace heating profile, given the ramp rates and braze temperatures were the same in the inert and reducing brazing profiles. In the cells brazed in reducing atmosphere, some minor colour change from grey to green was observed around the tips of the

Table 1
Electroless nickel-phosphorus braze material vs BNi-7 property and brazing temperature.

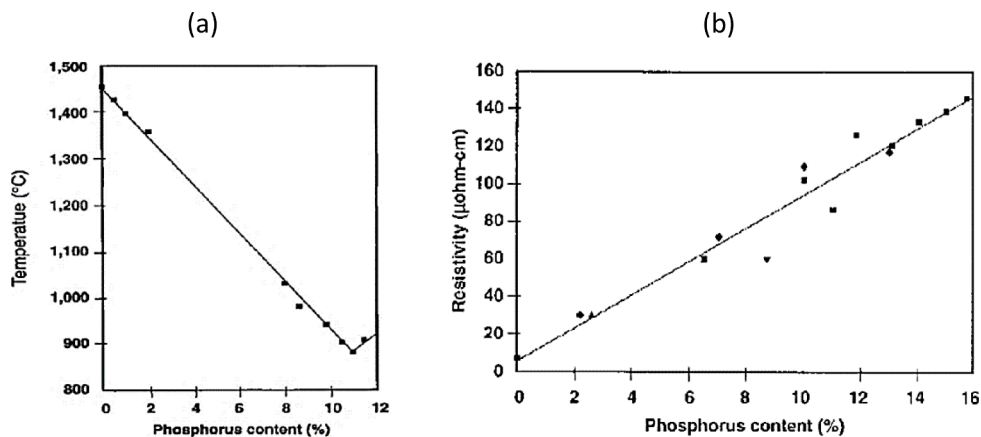| Product Name AWS A58	Ni (wt%)	Cr (wt%)	Fe (wt%)	B (wt%)	Si (wt%)	P (wt%)	Brazing Range (°C)	Suggested Brazing Temperature (°C)
BNi-7	75.9	14	-	-	-	10.1	960-1127	1065
Electroless Ni-P Braze	Bal	-	-	-	-	6.0-9.0	900-1100	1060

(a)

(b)

Fig. 2. Phosphorous content versus (a) melting point, and (b) versus electrical resistivity of the EN alloy (Parkinson, 1997).
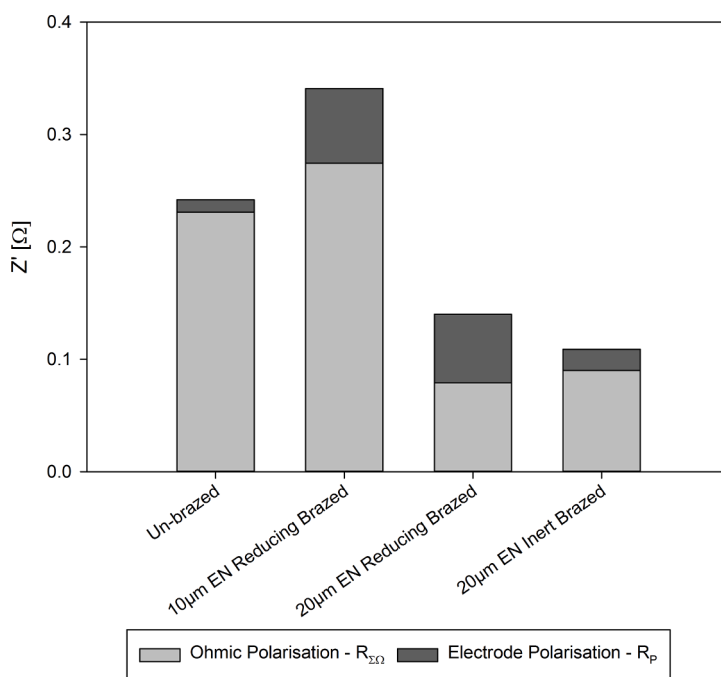

Fig. 3. Ohmic resistance at 0.7 V of cells with hiTRAN® elements un-brazed versus brazed in inert and reducing atmospheres.

anode, indicating some re-oxidation had occurred. The electrode polarisation values indicated that overall, an inert environment was more beneficial. Indeed, the cells with the lowest total resistance were the cells brazed in inert conditions. The ASR values with hiTRAN® elements as the current collector were 4.77 $\Omega.cm^2$, 6.19 $\Omega.cm^2$, 2.76 $\Omega.cm^2$ and 2.15 $\Omega.cm^2$ for the cells with un-brazed hiTRAN® turbuliser, the 10 μm EN and 20 μm EN coated hiTRAN® brazed in a reducing environment, and the 20 μm EN hiTRAN® brazed under inert conditions, respectively.

If brazing half cells (anode and electrolyte, without cathode), it would be preferential to braze in a reducing environment. The cathode could then be prepared in a later process, taking care to select the sintering environment appropriately, ideally using a reducing environment on the anode side and an oxidising (air, typical in the cathode sintering process) or inert environment (nitrogen) on the cathode side.

The polarisation and power plot of the cells with hiTRAN® current collector un-brazed, brazed in reducing atmosphere with 10 μm EN and 20 μm EN plating, and with 20 μm EN plating brazed in an inert environment, are seen in Fig. 4. The lower current density at 0.7 V, lower peak power and higher estimated ASR of the hiTRAN® with 10 μm EN coating brazed in reducing conditions as compared to the un-brazed cell confirmed the findings from impedance spectroscopy. The loss of performance was attributed to an increase in both ohmic polarisation and electrode polarisation, the former from the increased contact resistance between the hiTRAN® and the anode, and the latter from the degradation of the cathode. Brazing in an inert and reducing environment led to the successful joining of the hiTRAN® and the anode at all points of contact when the thickness of EN braze was increased to 20 μm. The physical joints resulted in relatively lower contact resistance between the hiTRAN® and the tube wall. This led to ASR values lower and a peak power density higher than with the un-brazed cell, even though the electrode polarisation increased in both cases.

Even though the total cell resistance (measured by EIS) was 28% higher for the cell with the 20 μm EN plated element brazed in reducing conditions, as compared to the 20 μm EN coated element brazed in inert conditions, the lower ohmic polarisation of the former led to superior cell performance overall. A summary of the electrochemical performance from this study is seen in Table 2.
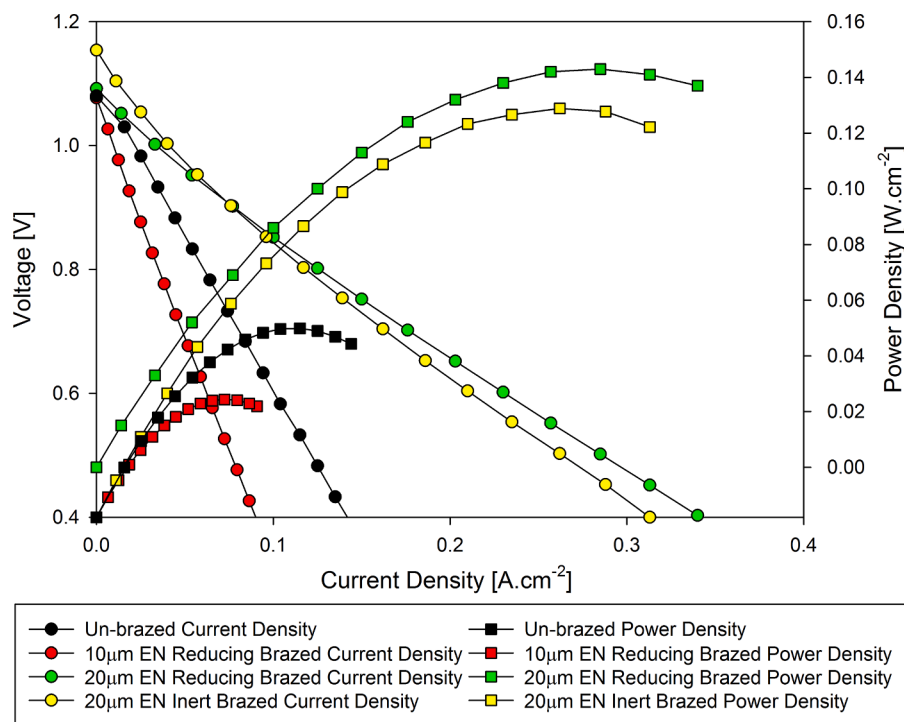
Fig. 4. Polarisation and power density plot with hiTRAN® as a current collector: un-brazed, 10 μm EN reducing brazed, 20 μm EN reducing brazed, and 20 μm EN reducing brazed at 750°C with a 200 ml.min^{-1} H$_2$ and 10 ml.min^{-1} N$_2$ gas flow rate.

Table 2
Summary of electrochemical data from cell tests with un-brazed versus brazed hiTRAN®.

	Electrode Polarisation [Ω]	Ohmic Polarisation [Ω]	ASR (EIS) [Ω. cm^2]	ASR (IV) [Ω. cm^2]	Current Density at 0.7 V [A.cm^{-2}]	Peak Power Density [W. cm^{-2}]
Un-brazed hiTRAN	0.011	0.231	4.77	5	0.079	0.061
10 μm EN Reducing	0.067	0.275	6.19	7.34	0.048	0.038
20 μm EN Reducing	0.061	0.079	2.76	1.94	0.176	0.143
20 μm EN Inert	0.019	0.09	2.15	2.22	0.162	0.132

Conclusion

Brazing was utilised for contacting a brush-like current collector named hiTRAN® at multiple points along the interior wall of an anode supported μT-SOFC. The high-surface area and tight-fitting, spring-loaded hiTRAN® turbuliser posed difficulties surrounding braze loading. To combat this, a novel electroless plated nickel-phosphorous braze was developed as a simple solution to braze loading at an industrial scale. Two braze coating thicknesses were trialled with a 20 μm coating identified as the minimum thickness required for forming a joint at every contact point. The 20 μm braze loading of EN braze, applied in both an inert and reducing environment all outperformed the non-brazed hiTRAN® current collector. From EIS measurements it was determined that an inert brazing environment led to lower electrode polarisation values while a reducing brazing environment favoured a lower ohmic polarisation and a higher quality anode-electrode joint. The design achieved an OCV above 1 V, a current density at 0.7 V of 0.176 A. cm^{-2} and a peak power density of 0.143 W.cm^{-2} at 750°C. The peak power density was 2.35 times higher than for the un-brazed design. The EN brazed hiTRAN® current collector design was deemed suitable for mass production and well suited for adoption in durable portable μT-SOFC stacks.

Declaration of Competing Interest

I can confirm that there are no conflicts of interest for all authors regarding the submission of the manuscript entitled 'Micro-Tubular Solid Oxide Fuel Cell Current Collector Contacting'.

References

Larmine, J., Dicks, A., 2006. Fuel Cell Systems Explained. John Wiley & Sons, Chichester, England.

Mench, M.M., 2008. Fuel Cell Engines. John Wiley & Sons, Hoboken, USA.

O'Hayre, R., Cha, S.-W., Celella, W., Prinz, F.B., 2009. Fuel Cell Fundamentals, Second. John Wiley & Sons, New York, USA.

Kendall, K., Kendall, M., Sui, S., Xiu, G.H., 2016. Fuels and fuel processing in SOFC applications. High-Temperature Solid Oxide Fuel Cells 21st Century. Elsevier, London, England, pp. 461–495.

Bujalski, W., Dikwal, C.M., Kendall, K., 2007. Cycling of three solid oxide fuel cell types. J. Power Sources 171, 96–100. https://doi.org/10.1016/j.jpowsour.2007.01.029 doi:

Kendall, K., 2016. Introduction to SOFCs, in: High-Temperature Solid Oxide Fuel Cells 21st Century. Elsevier, London, England, pp. 1–24.

Kendall, K., Kendall, M., Kendall, K., 2016. High-Temperature Solid Oxide Fuel Cells 21st Century. Portable early market SOFCs. Elsevier, London, England, pp. 329–356.

Meadowcroft, A., Howroyd, S.R., Kendall, K., Kendall, M., 2013. Testing microtubular SOFCs in unmanned air vehicles (UAVs). ECS Trans. 57, 451–457. https://doi.org/10.1149/05701.0451ecst doi:

Fernandes, M.D., de, S.T., Bistritzki, V.N., Fonseca, R.M., Zacarias, L.G., Gonçalves, H.N.C., de Castro, A.F., Domingues, R.Z., Matencio, T., 2018. SOFC-APU systems for aircraft: A review. Int. J. Hydrogen Energy 43, 16311–16333. https://doi.org/10.1016/j.ijhydene.2018.07.004 doi:

Lee, S.-B., Lim, T.-H., Song, R.-H., Shin, D.-R., Dong, S.-K., 2008. Development of a 700 W anode-supported micro-tubular SOFC stack for APU applications. Int. J. Hydrogen Energy. https://doi.org/10.1016/j.ijhydene.2008.02.034 doi:

Boersma, R.J., Sammes, N.M., Fee, C.J., 2000. Losses resulting from in-plane electricity conduction in tubular solid oxide fuel cells. Solid State Ionics 135, 493–502.

Panthi, D., Tsutsumi, A., 2014. Micro-tubular solid oxide fuel cell based on a porous yttria-stabilized zirconia support. Sci. Rep. 4, 1–6. https://doi.org/10.1038/srep05754 doi:

Hodjati-Pugh, O., Andrews, J., Dhir, A., Steinberger-Wilckens, R., 2021. Analysis of current collection in micro-tubular solid oxide fuel cells: An empirical and mathematical modelling approach for minimised ohmic polarisation. J. Power Sources 494, 229780. https://doi.org/10.1016/j.jpowsour.2021.229780 doi:

Dhir, A., Kendall, K., 2008. Microtubular SOFC anode optimisation for direct use on methane. J. Power Sources 181, 297–303. https://doi.org/10.1016/j.jpowsour.2007.11.005 doi:

Bai, Y., Wang, C., Jin, C., Liu, J., 2011. Anode Current Collecting Efficiency of Tubular Anode-supported Solid Oxide Fuel Cells. Fuel Cells 11, 465–468. https://doi.org/10.1002/fuce.201000053 doi:

Hodjati-Pugh, O., Dhir, A., Steinberger-Wilckens, R., 2021. The development of current collection in micro-tubular solid oxide fuel cells—a review. Appl. Sci. 11, 1–27. https://doi.org/10.3390/app11031077 doi:

Majewski, A.J., Dhir, A., 2018. Application of silver in microtubular solid oxide fuel cells. Mater. Renew. Sustain. Energy 1–13. https://doi.org/10.1007/s40243-018-0123-y doi:

Dhir, A., Kendall, K., 2007. Improving Reliability of Microtubular SOFCs for Direct Use on Methane. ECS Tran. 7, 823–828. https://doi.org/10.1149/1.2729171 doi:

Hodjati-Pugh, O., Dhir, A., Steinberger-Wilckens, R., 2021. Internal current collection and thermofluidynamic enhancement in a microtubular SOFC. Int. J. Heat Mass Transf. 173 https://doi.org/10.1016/j.ijheatmasstransfer.2021.121255 doi:

A. Meadowcroft, K. Howe, A. Dhir, R. Steinberger-Wilckens, Connection Optimisation for Micro-Tubular Solid Oxide Fuel Cells (A1507), in: 11th Eur. SOFC SOE Forum, Lucerne Switzerland, 2014.

Fergus, J.W., 2005. Metallic interconnects for solid oxide fuel cells. Mater. Sci. Eng. A 397, 271–283. https://doi.org/10.1016/j.msea.2005.02.047 doi:

Kendall, K., Kendall, M., Niewolak, L., Tietz, F., Quadakkers, W.J., 2016. Interconnects, in: High-Temperature Solid Oxide Fuel Cells 21st Century. Elsevier, London, England, pp. 195–254.

Kim, J.H., Song, R.H., Shin, D.R., 2009. Joning of metallic cap and anode-supported tubular solid oxide fuel cell by induction brazing process. J. Fuel Cell Sci. Technol. 6, 0310121–0310126. https://doi.org/10.1115/1.3006344 doi:

Erskine, K.M., Meier, A.M., Pilgrim, S.M., 2002. Brazing perovskite ceramics with silver/copper oxide braze alloys. J. Mater. Sci. 37, 1705–1709.

Mahato, N., Banerjee, A., Gupta, A., Omar, S., Balani, K., 2015. Progress in material selection for solid oxide fuel cell technology: A review. Prog. Mater. Sci. 72, 141–337. https://doi.org/10.1016/j.pmatsci.2015.01.001 doi:

Tucker, M.C., Jacobson, C.P., De Jonghe, L.C., Visco, S.J., 2006. A braze system for sealing metal-supported solid oxide fuel cells. J. Power Sources 160, 1049–1057. https://doi.org/10.1016/j.jpowsour.2006.02.067 doi:

Chao, C., Chu, C., Fuh, Y., Hsu, R., Lee, S., Cheng, Y., 2016. Joint strength of Ag –9Pd –9Ga brazed interconnect and anode-supported electrolyte for solid-oxide fuel cell applications. J Mater. Des. Appl. 0, 1–12. https://doi.org/10.1177/1464420716647077 doi:

Sammes, N.M., Du, Y., Bove, R., 2005. Design and fabrication of a 100 W anode supported micro-tubular SOFC stack. J. Power Sources 145, 428–434. https://doi.org/10.1016/j.jpowsour.2005.01.079 doi:

Hodjati-Pugh, O., Dhir, A., Steinberger-Wilckens, R., 2019. Internal Current Collection in Microtubular SOFCs : Minimisation of Contact Resistance via Brazing and Plating. ECS Trans. 91, 553. https://doi.org/10.1149/09101.0533ecst. –548doi:

Sudagar, J., Lian, J., Sha, W., 2013. Electroless nickel, alloy, composite and nano coatings - A critical review. https://doi.org/10.1016/j.jallcom.2013.03.107 doi:

Parkinson, R., 1997. Properties and applications of electroless nickel. Nickel Dev. Inst. 37. https://www.nickelinstitute.org/media/1769/propertiesandapplicationsofelectrolessnickel_10081_.pdf (accessed February 5, 2020).

D. Sekulic, Advances in Brazing: Science, Technology and Applications, Woodhead Publishing, 2013.